P- ISSN 1991-8941E-ISSN 2706-6703
2021,15 (1) :37 – 48

Journal of University of Anbar for Pure Science (JUAPS)

Open Access

Experimental and Theoretical Study of Parabolic Trough Solar Collector Performance Without Automatic Tracking System

Khudir Zidane Zarrag*[1], Fayadh M. Abed[2], Salim. Y. Kasim[2]

[1] Anbar Sewer Directorate, Anbar Province, Ramadi, Iraq
[2] Department of Mechanical Engineering, Faculty of Engineering, Tikrit University, Tikrit, Iraq

ARTICLE INFO
Received:10 / 4 /2021
Accepted: 15 /5/2021
Available online: 1/ 6/2021
DOI: 10.37652/juaps.2022.172430

Keywords:
Parabolic trough collector,
Thermal collector performance,
Solar energy

A B S T R A C T

In this research, a practical and theoretical study was conducted to evaluate the performance of parabolic trough collectors (PTCS) of length (3 m) and width (2.67 m) for three solar collectors connected in parallel, and the absorber tube is made of stainless steel with an internal and external diameter (0.028 m), (0.031 m), respectively. The absorber tube of length 11 m, was painted with un shiny black paint to increase the absorption of sunlight and reduces the thermal radiation. The working fluid is transferred through the receiver tube and located at the focus area of the three collectors. The collector width aperture width was 0.8 meters, and 2.40 meters length with rim angle of Ø = 90°, and concentration ratio of 8.02. The collector surface was covered with aluminum foil which is available in the local market (3M SA-85), which covers galvanized iron sheets with a thickness of 2 mm. A computer program in Fortran language was built to calculate the performance of the solar collector. Experimental results of the test showed that the performance factor of the solar collector is less than the typical type, where notes that there is a large deviation between the theoretical and experimental results, especially in the winter, where the deviation in the morning at ten o'clock about 78%, while it was 5% at noon. The large deviation value mentioned resulting from the assumptions that have been developed to simplify the equations that were used in the theoretical side of research, also the reasons that the theoretical results are taken on the assumption that weather conditions are clear sky and that contrary to reality in the winter. ٥The best efficiency of the solar collector was between solar time (12:00) and time (1:00) at night for two seasons, and the obtained results showed that the increase of mass flow rate of fluid from the amount of (0.033) kg/sec to the amount of (0.066) kg/sec increases the efficiency of solar collector, but leads to reduce the temperature difference between the inlet and exit, as well as the results showed that an increase in solar flux increases the useful energy obtained from the solar collector.

1. INTRODUCTION

God bless our country with renewable energy sources: sun, wind, biomass. Statistics show that Iraq receives the equivalent of solar energy more than 5,000 trillion (kWh/year), which is more than the total energy of the country's consumption, and that the average daily global radiation is about (5 kWh) per square meter per day and sunny hours range from 2,300 to 3,200 sunny hours per year[1]. There are three main types of solar collectors: flat collectors, concentrated collectors and evacuated tube collectors, each type contains different shapes, and each form has distinctive characteristics that make it suitable for some uses, and we will address the type of our study:

*Corresponding author at: Ramadi Municipality Directorate, Anbar Sewer Directorate – Iraq;E-mail address: eng_khudir@yahoo.com

2. PARABOLIC TROUGH COLLECTOR

Parabolic trough collector consisting of moving reflective surface and a fixed tube that passes along the focal line as in Figure 1.2. The reflective surface is located and takes the form of a part of a cylinder, the reflective surface focuses the fallen rays on the liquid-carrying tube, and moves this surface to follow the sun's daily movement.

Parabolic Trough collector is the best type with respect to collectors [2] because of its ability to operate at high temperatures and give high efficiency. Compound Parabolic Collector [3] operates at an efficiency of about 32% and flat plate solar collector [4] at about 10%, therefore parabolic trough collectors are used in many engineering applications, such as steam generation for industrial applications [6], Power generation [7,8], domestic heating, and desalination of seawater [9,10].

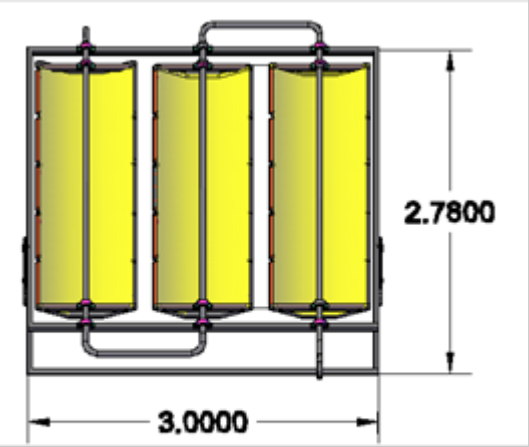

Fig (1) Top view

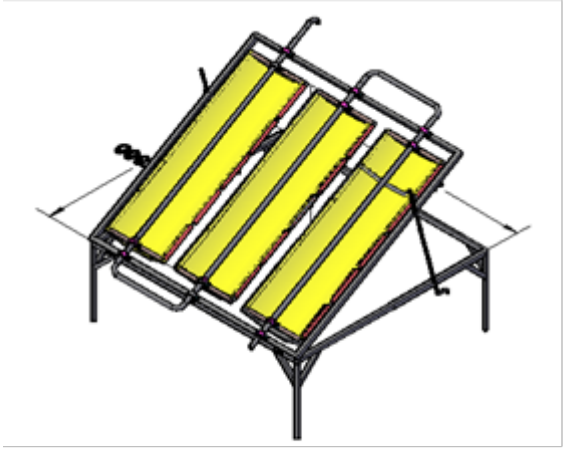

Fig(2) Three Dimensional

Most of the published studies in the subject of parabolic trough collector aimed at generating electricity by focusing solar rays on the absorber tube (fluid-bearing tube) which used in the solar power plants (SEGS) [11,12]. Most studies have also focused on the use of industrial oil as a major fluid passing through a tube located at the center of the solar radiation-focused inverter.and after the working fluid is heated, it passes on another heat exchanger carrying water intended to convert it into water vapor for use in steam turbines. The use of such oils is associated with a number of industrial problems, such as toxicity, ignition, thermal instability and high cost [13]. In 1992, Dagan *et al.* [14] and Lippke [15] proposed three concepts for a DSGC system. which is to generate Super-heated steam in the first stage, and then recycling to generate wet steam and then injected into steam to control the quality of steam and unsteady flowing inside the absorbent tube.

In 1996, Kalogirou[16] designed parabolic trough collector with surface area of (3.5m^2) and rim angle of 90^o degrees and a concentration ratio (21.2) performance measurements performed in accordance with the Standard ASHRAE 93 (ASHRAE 1991). In the same year, Ibrahim [17] used six connected parabolic collectors, each of them with a length of (1.14m) long and wide (0.12m) and a total area of (0.82m^2). In 1997, Almanza and Jimenez [18] were able to get steam from using a 29-meter-long absorbent tube installed in the focus of the parabolic trough collector with an opening width of (2.5m) and a diameter of (25.4mm).

In 1999, Bakos et al. [19], using a 12-square-meter parabolic trough collector with two axes tracking technology for the purpose of monitoring the movement of the sun and obtaining a high radiation concentration. In 2001, Singh and Sulaiman [20] were able to calculate the heat transfer coefficient on the surface of the fluid-bearing tube used in solar centers, which plays a major role in calculating the performance efficiency of the solar collector, where it was able to establish a mathematical relationship by finding a remote factor as a temperature function instead of a dynamic viscosity factor, and as a result able to calculate the effect of the diameter of the fluid-bearing tube on the speed of fluid flow, at water temperatures ranging from 0 to 360°C and at a constant mass flow rate.

In 2008, Derek Lipp [21] conducted an experimental study to find the best focal length and best width in the parabolic solar collectors based on the value of solar radiation.

In 2010, TadamunYasin Ahmed [22] studied the thermal performance of parabolic trough collectors. The solar collector was (1.9 m) long, 1 m width, and used a heat absorbent tube with an internal diameter (0.026 m) and an external diameter (0.03 m) with water as heat transfer fluid. The experimental study was completed during the summer and winter in Tikrit, Iraq. Solar radiation for Tikrit, calculated theoretically. The theoretical study was completed using the Fortran 90 program, specifications and dimensions of the solar collector injected into the program to calculate theoretical thermal efficiency. The practical thermal efficiency of the solar collector was found to be 7-15 % lower than the theoretical efficiency. The increase in mass flow rate was led to an increase in thermal efficiency.

The current study used three receivers, each with a length of (2.4m), and width (0.8m) and a total area of (5.76m^2). Absorbent tube length (11m), diameter (31.75 mm) and rim angle (90) degrees. The concentration ratio (25.19). The measurements were made in accordance with ASHRAE 93 (ASHRAE 1991).

3. EXPERIMENTAL PART

The parabolic solar collector model is designed and manufactured in the laboratories of the Department of Mechanical Engineering, Tikrit University). As described in diagrams No. (1), and (2), photographs (3) and (4), according to the engineering specifications described in table (1). In order to ensure that the sunlight falls on all areas of the collectors during the test, the distance between

the collectors is limited to (20 cm), where the distance between the centers of collectors is (100 cm), the width of the collector (80 cm), so the distance between the ends of each collectors not exceed (20 cm) and this is sufficient distance to avoid interference.

Table (1) Engineering specifications for the solar collector

Subject	Value
(Collector aperture area)	5.76 m^2
Collector aperture)(	0.8 m
(Rim angle)	°90
(Receiver diameter)	31.75 mm
(Tracking mechanism type)	Manual
(Mode of tracking)	North-South, Horizontal
(Concentration ratio)	25.19

Fig (3) Front view

Fig (4) Side view

The locally manufactured collectors his diagram is shown in figure (1) and (3) consists of eight main parts:

3.1. Iron Fram

It is a structure of 3m -long and 2.8m width, and the structure was made of lightweight square iron sections for easy installation and binding in the required places and mounted with screw joints and columns that allows the tilt angle to be changed according to the angle of latitude as shown in figure (2) and (3). The tilt angle control mechanism is shown on both sides in order to get rid of vibrations and get a steady and balanced movement, knowing that the control mechanism is a serrated rod mounted on the same to give the user the freedom to choose the angle of inclination according to the design prepared for it.

3.2. Solar Collectors

Solar collectors are made from galvanized iron plates designed to give a suitable and calculated focal length, formed by roller devices according to the design dimensions of the collectors to ensure the reflection of sunlight to the focal line. Aluminum foil sheets have been installed with high reflectiveness and according to what is available in the local markets on the concave part of the collectors to reflect the solar rays on the focal line, which represents the absorbent tube (carrying fluid). The plate is installed on an iron structure to get a coherent collector and remain constant during the test.

The manual tracking mechanism is a serrated rod similar to the tilt angle control mechanism with high flexibility to reverse the direction of the solar collectors and track the movement of the sun from east to west and as shown in figure (4). The nature of soft teeth has been chosen to allow us to control accurately and direct the collectors with precise mechanical motion so that we can maintain the concentration of solar rays towards the focal line and throughout the test period to get the right results.

3.3. Absorbent Tube

The tube, represent the important part, for the system. It is made from stainless steel with diameter of (31.75mm), and length (11m). The tube passage along the length of the focal line and fixed by screws on the steel frame. Thermocouples are installed at the inlet and exit vents. Flow meter was installed before the inlet vent to control the flow rate through a lock diameter (12) mm and a check valve diameter (31.75) mm to prevent the return of the fluid to the inlet as shown in figure (7), also a lock of diameter (12) mm was installed in the outlet hole to precisely control the amount of fluid flowing from the tube carrying the fluid to the outside, the tube was coated with a matte black dye to increase the absorbency of the tube. The tube was also isolated from the space between the collectors to reduce thermal loss.

3.4. Flow meter

It is a flow measuring device with gradations of (0.4 - 4) liters / minute as shown in picture (5). A measuring ruler was used to mark small flows of fluid that are less than (0.4) liters / minute and their accuracy was confirmed by conducting experimental readings by calculation of the quantities of fluid exiting during a unit of time for different flow quantities.

3.5. Thermocouple

It is a thermocouple (type k) to measure the temperature of the fluid at the inlet and outlet vents of the absorbent tube (the fluid carrying) as shown in Figure (7), where these thermocouples were connected by special channels linked to a computer and located inside iron box near the system. The readings were recorded by computer via the thermal monitoring system program and stored on computer files after entering the required data of air temperature, testing periods, and reading periods.

The thermocouple heads were installed into the holes that drilled especially in the walls of the absorbent tube (the fluid carrying) by nuts with the same diameter of the thermocouple and then welded to the inlet and exit holes by special welding of stainless steel, and its depth was suitable to be in the center of the tube. The temperature of the fluid in the inlet and exit holes was measured using a digital thermal monitoring system. The ambient temperature, in addition to measuring it using this device, was also measured using a mercury thermometer with a range of 100 degrees Celsius and with an accuracy of 0.1 degrees Celsius.

3.6. Thermal Control System

It is an electronic board that was manufactured from a group of registers, thermal resistors, integrated circuits (I.c.), and electronic filters, all of which were attached to a Visa type electronic board installed in one of the slots of the expansion slots in the motherboard inside a tabletop computer. The control system was installed inside a thermally insulated iron box to ensure the continuity of electrical current during the testing periods, where the

Fig (6) Computer, inverter, System battery charging

Fig (7) Thermometer (thermocouple), anti-return valve

computer was connected to an inverter and a charging battery that lasts for 8 hours, as shown in Figure (6). The computer, through the thermal monitoring system program, records the temperature readings of the fluid in the inlet and exit area by the thermocouples connected to the computer via an electronic board containing 16 channels, as it has the ability to measure the temperature of each thermocouple directly and with an accuracy of 0.1 ° C, where the readings are taken automatically and during specified periods by the user and during specific hours as well. The arrangement of the channels is in the form of opposite pairs and each pair contains a positive terminal and other negative.

3.7. Tracking Mechanism Type

It consists of a toothed rod, fixing nuts and guide arms, as shown schematically in figure (2) and (4). It has been designed with smooth teeth to provide accurate and easy movement during the process of tracking sun movement from east to west, where movement and change of direction are uniform for all collectors in order to obtain a permanent focus of the solar rays towards the focal line, and by the same mechanism the angle of inclination of the receiver is changed and it is designed to be from two sides in order to avoid the vibrations that may occur during the experimental tests.

4.Thermal Efficiency Calculation

The measurement and testing of thermal efficiency depends on the increase in the fluid temperature difference between

the inlet and outlet vents of the tube and on the direct solar radiation (GDN) data which is measured at the same time as the temperature difference is measured. In such designs and tests, they are usually conducted for a period of ten or five minutes and from these readings the amount of thermal efficiency is calculated. The efficiency of parabolic trough solar collector (PTC) is calculated experimentally by dividing the amount of energy absorbed in the fluid that flows inside the tube (Receiver) on the amount of energy incident on the area of the receiver, which is expressed in the following formula [23]:

$$\eta_g = \frac{\dot{m}.C_p\left(T_{fo} - T_{fi}\right)}{G_{bp}..A_a} \qquad \ldots\ldots\ldots\ldots\ldots \quad (1)$$

whereas:

(A_a): represents the collector aperture area.

(G_{bp}): represents the direct solar radiation component falling on the area of the receiver, which depends on the calculation of the incidence angle of solar radiation (θ_i) and the value of direct radiation (GDN) measured practically using the port lock system, which is a device that has the ability to measure weather conditions variables from direct solar radiation, wind speed, relative humidity, and air temperature.

The value of solar radiation is calculated at each time period due to the difference in the amount of solar radiation and the angle of incidence of the sun.

$$G_{bp} = G_{DN}.\cos\theta_i$$

Where: (θ) represents the angle of incidence of the sun.

(A_a): represents the area of the three collectors and its value (5.76 m^2).

($\dot{m}$): represents the rate of mass flow of fluid entering the solar collector.

(T_{fo} - T_{fi}) represents the temperature difference between the inlet and outlet of the fluid-carrying tube, and is practically measured by thermocouples, as mentioned previously.

As for the specific temperature (Cp) of the fluid, it is calculated directly from the tables of the physical specifications of the water and at each time period and at the average temperature between entry and exit.

As for the rate of thermal energy absorbed by the fluid ($C_p\Delta t$), it is also calculated at each measurement period and depending on the difference in temperature of the fluid between inlet and exit, and at the specific temperature values of the fluid and for each flow rate.

It is worth noting that when conducting tests and practical calculations for the solar radiation component and calculating the angle of incidence of solar radiation, it was found that its value most of the time = zero or close to zero, and in the worst cases even in the winter when the sun is low, we found that the solar radiation component is approximately equal to the value of radiation. The measured solar system is practically measured and for the same time and conditions. The reason is that the tracking process of the sun's disk is conducted with two axes from east to west and the axis of the angle of inclination of the collector that is changed every test day according to the solar incidence radiation which is changed along the year. Thus, the orthogonal fall of the solar rays towards the receiver is preserved, so the practical solar radiation values have been adopted in the calculation of the thermal efficiency as follows:

$$G_{bp} = G_{DN}.\cos\theta_i$$
$$G_{bp} = G_{DN}.\cos(0) = G_{DN} \times 1 = G_{DN}$$
$$\therefore G_{bp} \approx G_{DN}$$

Table (2) shows a mathematical model for thermal efficiency, where the obtained results represent the data that go into calculating the thermal efficiency. The columns in the aforementioned table represent the practically measured data for fluid temperatures in inlet and exit and solar radiation, as well as represent the practically measured data for wind speed and relative humidity for the test days. The thermal efficiency of the first row in the table will be calculated as an illustration of the calculations that took place during the test months of 2019. The average temperature of the fluid is extracted as follows:

$$T_{ave} = \frac{\left(T_{fo} + T_{fi}\right)}{2} = \frac{(16.00 + 17.05)}{2} = 16.525\ ^{\circ}\text{C}$$

At this temperature, the specific water temperature (C_P) is calculated by using the tables for the physical specifications of the water.

C_P = 4186.72 (J / kg. k)

Thus, when dividing the total energy absorbed by the fluid to the total solar radiation on the surface of the receiver, the required thermal efficiency is calculated as follows:

$$\eta_g = \frac{\dot{m}.C_p\left(T_{fo} - T_{fi}\right)}{G_{bp}..A_a} = \frac{145.069}{1278.72} = 11.34\,\%$$

And so for the rest of the calculations that were practically calculated and for all days of the test.

Equation (1) is used to process practical data collected during the tests.

5. Theoretical Part

The numerical analysis method was used in the simulation procedure to determine the performance of the thermal model and solve the performance parameters of the solar collector. A computer program in Fortran language was built to obtain the results.

6. RESULTS and DISCUSSION

The experiments were conducted from 10:00 in the morning until 2:00 in the afternoon on all the different testing days and throughout the year and for the various seasons of the year 2012. The tests were conducted on days 7, 14, 21 and 28 of each month and for different flow rates and different water temperatures. It is entered into the absorbent tube, but it is worth noting that some days whose data were approved do not match those dates due to bad weather or some special circumstances that prevented testing on some days.

6.1 .Theoretical Results

As part of the study, the theoretical analysis method was used in the simulation to determine the performance of the solar collector to study the effect of forced convection resulting from the effect of fluid flow and the incident rays reflected on the receiver and focused on the absorbent tube. A computer program in the Fortran language was built to calculate the performance of the solar collector. Measurements were carried out at the conditions and limits that were determined and in accordance with the requirements of the proposed design. The results obtained gave a performance efficiency of (50%) in the winter at mass flow of (0.033) kg / s, while in the summer the efficiency values were close to the value of (54%) and for the same values of mass flow of fluid, which is an acceptable percentage within the designs for solar collectors.

6.2. Experimental Results

On the practical side, the thermal efficiency of the solar collector was calculated through the readings that were recorded by the aforementioned devices. The readings were recorded at a different mass flow at a value of (0.033) kilograms / second and a value of (0.066) kilograms/second.

The solar collector was tested with different weather conditions over nine months of 2019, as (900) readings were recorded for each of the variables included in the calculation of thermal efficiency in addition to the values of ambient temperatures, relative humidity values , and wind speed values at the same times in which the values were recorded. In this research, the values of solar flux, ambient temperature, and wind speed obtained from a Port log meteorology system were adopted for all test days and from 10:00 am to 2:00 pm.

6.3.Discussion and Comparison Of Theoretical And Experimental Results

To know the extent of congruence between the results obtained in the theoretical side with the results obtained in the practical side of this research, this comparison has been clarified through its representation in figures (8), (9), (10), and (11). The results showed an increase in the thermal efficiency when increasing the mass flow rate of the water entering the solar collector, and this is consistent with the experimental results as shown in figure (8), which shows a comparison between theoretical and experimental results for the values of thermal efficiency at a flow rate of (0.033) kg / s and a flow of (0.066)) kg/s in the winter season for 7 January 2019 and 21 January 2019, respectively.

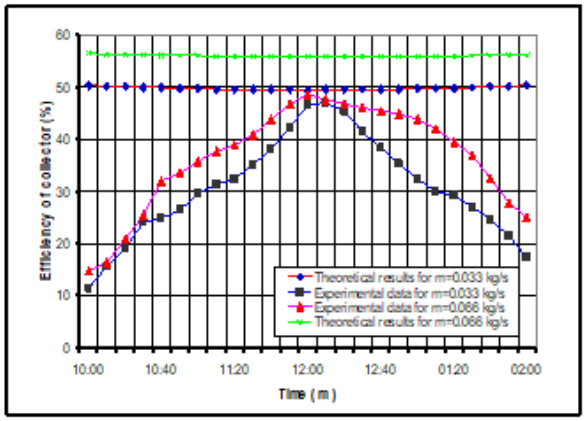

Figure (8) Comparison between theoretical and practical results for the values of thermal efficiency at a flow rate of (0.033) kg / s and a flow of (0.066) kg / s in the winter for 1/7/2019 and 21/1/2019 respectively

Figure (9) shows a comparison between the theoretical and experimental results of the values of solar radiation in the winter season on 7 January, 2019, where it is noticed that there is a large divergence between the values, as the deviation at ten in the morning reached (78%) while the deviation reached at twelve O'clock About (5%).

The aforementioned deviation ratio is due to the assumptions that were developed to simplify the solution of the equations that were used in the theoretical side of the research in terms of the dependence of the rates of values with respect to the temperature of the ocean, tube or fluid, As well as the theoretical solar radiation values that directly affect the efficiency values, as they are calculated theoretically without reference to practical devices that automatically record realistic readings.

The reason is also attributed to the fact that the theoretical results are taken on the assumption that the weather conditions are good and the sky is clear. This is in contrast to the reality in the winter season where there is a clear fluctuation in the values of solar radiation, as a result of the presence of clouds that lead to the dispersion of direct

solar radiation and change the rate of its values during the test period, although that days were chosen in good weather conditions.

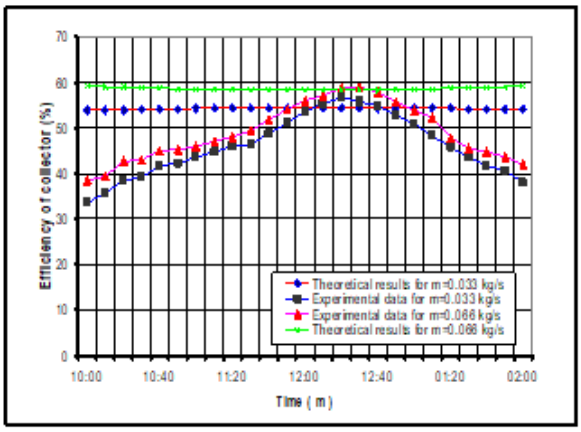

Figure (9) Comparison between theoretical and practical results for the values of thermal efficiency at (0.033) kg / s flow rate and (0.066) kg / s flow in the summer for 5/7/2019 and 14/5/2019, respectively

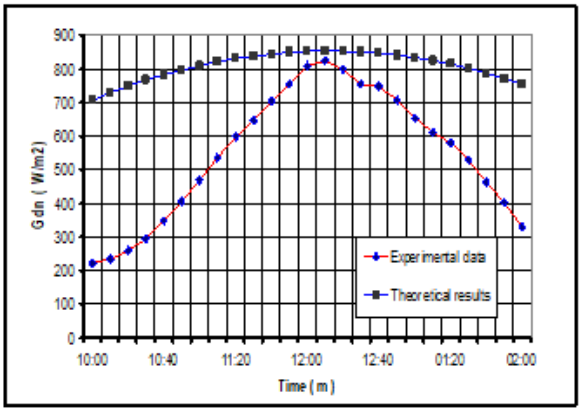

Figure (10) a comparison between the theoretical and practical results of the values of solar radiation in the winter season on 1/7/2019

In the summer season, the results were very close in terms of the values of solar radiation, as shown in figure (11), which shows the comparison between the theoretical and practical results of the values of solar radiation in the summer season on 5/5/2019, where there is a great convergence between theoretical and practical results. The reason is the convergence of the actual weather conditions in the summer with the conditions that were taken into consideration in the theoretical results in terms of clear sky, direct solar radiation, and the height of the sun disk.

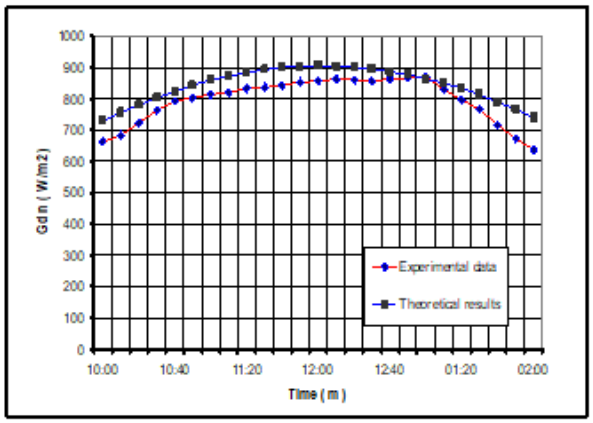

Figure (11) a comparison between the theoretical and practical results of the values of solar radiation in the summer season 5/7/2019

It is worth noting that the theoretical results were recorded and calculated at the average values for the variables included in the theoretical equations to calculate the performance of the solar collector in terms of the ambient temperature and the temperature of inlet and exit of water, as well as the values of solar radiation, which are theoretically calculated and their values automatically compensated by the computer program.

Discussing the experimental results in terms of solar radiation values, ambient temperatures, and thermal efficiency of the solar collector between winter and summer:

Table (2) shows a sample of the results of the process that were obtained in the winter season and on 7 January 2019, with a mass flow rate of (0.033) kg /s, and this table shows that the highest value of the solar flux was obtained is (823 W/m^2) and at the hour 12:10 As the solar radiation decreases with time according to a sinusoidal function. Figure (12) shows the temperatures of the ambient and of the water entering and leaving the absorbent tube on 1/7/2019.

Table (2) Practical measurements in the winter season for 1/7/2019 when a mass flow of water (0.033) kg / s

Test Time(s)	(T_{fi}) (°C)	(T_{fo}) (°C)	T_{amb} (°C)	G_{DN} (W/m^2)	Δ T (°C)	Hum (%)	Wind Speed	Efficiency (%)
10:00	16.00	17.05	9	222	1.05	84	2.7	11.34
10:10	16.50	18.15	9.1	255	1.65	82	3.2	15.55
10:20	17.00	19.25	9.4	281	2.25	80	3.2	19.18
10:30	18.0	21.20	9.6	318	3.20	79	3.0	24.11
10:40	19.4	23.01	10.0	350	3.61	78	2.8	24.78
10:50	20.5	24.99	10.2	406	4.49	80	3.0	26.51
11:00	20.9	26.60	11	460	5.70	79	3.6	29.69
11:10	21.0	28.01	11.2	536	7.01	78	3.6	31.35
11:20	21.2	29.33	11.6	600	8.13	77	3.5	32.46
11:30	21.3	30.78	12.3	645	9.48	76	3.7	35.21
11:40	21.4	32.63	13.0	705	11.23	75	4.2	38.15
11:50	21.4	34.70	13.8	755	13.30	68	4.0	42.24
12:00	21.6	37.31	15.0	808	15.71	65	4.0	46.57
12:10	21.6	37.73	14.6	823	16.13	60	3.6	46.94
12:20	21.7	36.82	15.3	798	15.12	56	3.6	45.38
12:30	21.7	34.79	15.8	755	13.09	49	3.5	41.53
12:40	21.7	33.65	16.4	748	11.95	47	3.6	38.29
12:50	21.7	32.15	16.5	708	10.45	46	3.3	35.36
01:00	21.8	30.50	16.5	653	8.80	46	3.0	32.29
01:10	21.8	29.48	16.6	612	7.68	44	2.9	30.07
01:20	21.8	28.88	16.7	580	7.08	43	3.0	29.24
01:30	21.8	27.76	16.8	528	5.96	43	3.6	27.05
01:40	21.6	26.34	17.0	462	4.74	42	3.7	24.60
01:50	21.4	25.00	17.2	402	3.60	39	3.5	21.46
02:00	21.4	23.80	17.2	330	2.40	38	3.8	17.44

Table (3) shows a sample of the results obtained in the summer and on 7 May 2019 with a mass flow rate of (0.033) kg/s. This table shows that the values of solar radiation and ambient temperature are much higher than those days in the winter season, and thus the increase in the water temperature, as it was significantly higher, which led to obtaining a relatively higher efficiency from the winter season, as the efficiency improved well. The reason is attributed to the lack of thermal losses from the absorbent tube due to the high temperatures of the ocean

Table (3) Practical measurements in summer for 5/7/2019 when a mass flow of water (0.033) kg / **s**

Test Time(s)	(T_{fi}) (°C)	(T_{fo}) (°C)	T_{amb} (°C)	G_{DN} (W/m²)	Δ T (°C)	Hum (%)	Wind Speed	Efficiency (%)
10:00	22.8	32.14	28.5	665	9.34	17	0.5	33.65
10:10	23.0	33.18	28.6	682	10.18	16	2.9	35.76
10:20	23.3	34.97	28.7	725	11.67	16	2.6	38.56
10:30	24.5	37.02	28.9	765	12.52	15	2.8	39.22
10:40	24.9	38.73	29.0	792	13.83	15	2.5	41.84
10:50	25.0	39.18	29.2	804	14.18	14	3.2	42.26
11:00	25.0	39.81	29.3	812	14.81	13	0.8	43.69
11:10	25.0	40.34	29.4	820	15.34	13	3.4	44.82
11:20	25.5	41.44	29.5	832	15.94	13	3.0	45.90
11:30	25.5	41.74	29.5	838	16.24	14	2.9	46.44
11:40	25.5	42.66	29.6	844	17.16	13	2.8	48.72
11:50	25.5	43.71	29.7	852	18.11	14	2.8	51.20
12:00	25.5	44.75	29.8	858	19.25	14	0.9	53.76
12:10	25.5	45.36	30.0	862	19.86	14	3.2	55.20
12:20	25.5	45.88	30.2	860	20.38	15	3.2	56.78
12:30	25.5	45.45	30.2	856	19.95	14	3.0	55.84
12:40	25.6	45.40	30.4	865	19.80	15	3.0	54.84
12:50	25.6	44.71	30.4	868	19.11	16	2.9	52.74
01:00	25.6	44.06	30.4	870	18.46	16	1.3	50.84
01:10	25.6	42.36	30.0	831	16.76	16	2.7	48.33
01:20	25.7	40.94	29.6	797	15.24	15	2.6	45.83
01:30	25.7	39.67	29.2	768	13.97	14	2.6	43.58
01:40	25.6	38.07	28.6	716	12.47	13	2.6	41.73
01:50	25.7	37.12	28.4	674	11.42	12	2.4	40.62
02:00	25.7	35.83	28.0	638	10.13	12	1.0	38.05

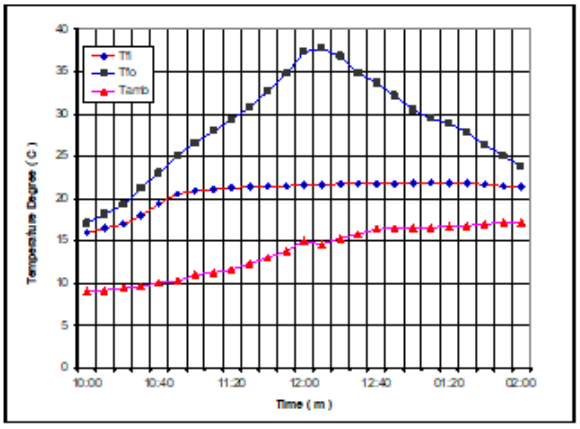

Figure (12) the temperatures of the ocean and the water entering and leaving the solar collector for

Figure (13) shows the temperatures of the ocean and the incoming and outgoing water from the solar collector recorded during the same test hours of 5/7/2019.

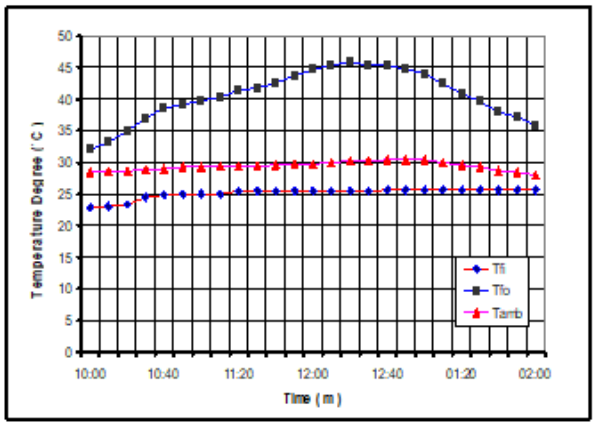

Figure (13) the temperatures of the ocean and the incoming water from the solar collector for 5/7/2019

Figure (14) shows a comparison of the solar radiation values between the winter and summer seasons of 2019, which shows the high average values of solar flux during the summer season, which is attributed to the increase in sunlight hours and the high angle of incidence of sunlight, so that it is almost vertical at the site in which the test was carried out, which is mainly due to change the movement of the earth and change the axis of rotation of the earth around itself.

The useful energy obtained from the collector increased from 10:00 to reach its highest value between 12:00 and 1:00 hours, coinciding with the increase in the solar flux as shown in figure (14), then it returns to decrease with the decrease in the solar flux. We note the same case with the rest of the thermal parameters and for both seasons of the year.

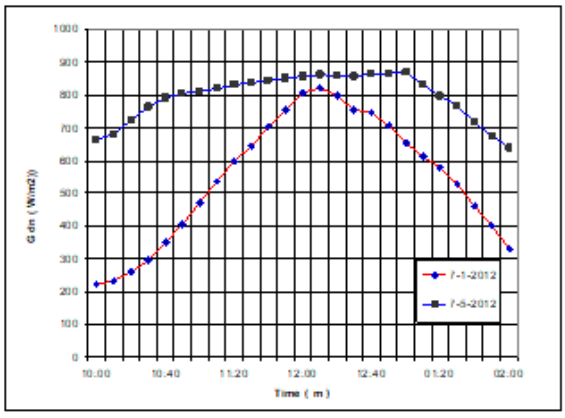

Figure (14) Comparison of the solar radiation values recorded in the winter and summer seasons

Figure (15) shows a comparison between the calculated thermal efficiency values in the winter and summer seasons at the same flow rate of water entering the solar collector, where the calculated thermal efficiency values are significantly higher in the summer and the reason

is due to the high temperatures and the lower values of the thermal losses.

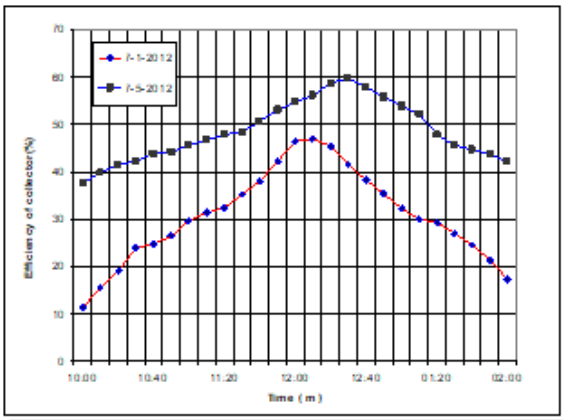

Figure (15) Comparison of thermal efficiency values calculated in winter and summer for the year 2019

6.4.Comparison of Experimental Results in Terms of Change of Mass Flow Rate

The change of the mass flow rate and its effect on the thermal efficiency values of the solar collector and its effect on the temperatures of the water entering the solar collector were studied, and the tests were conducted for the winter and summer seasons, where the change of the mass flow rate of the water entering the solar collector was tested for almost similar weather conditions, and it was found that the thermal efficiency of the solar collector increases with the increase in the flow rate of the water entering the absorbent tube and as shown in figure (16), which shows a comparison between the values of the thermal efficiency of different flow rates during the winter season where the thermal efficiency increased significantly from the increase in the mass flow rate of the fluid and the reason is attributed to the increased improvement in heat transfer. The absorption of thermal energy increases by the water flowing through the absorbent tube due to the increase in the velocity of the water.

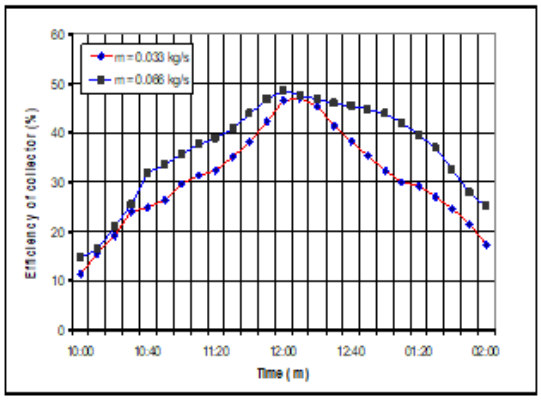

Figure (16) The efficiency of the solar collector at a different mass flow rate of the incoming water for the month of January 2019

However, the increase in the mass flow rate of the water entering the solar collector has led to a decrease in the temperature difference between the entrance and exit hole of the absorbent tube (receiver), as shown in Figure (17).

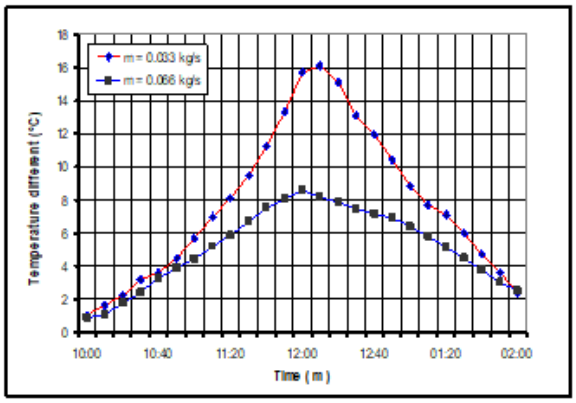

Figure (17) The difference in temperature between the inlet and outlet openings of the absorbent tube at a different mass flow rate of the water entering the solar collector for January 2019

Likewise, a test of changing the mass flow rate of the water entering the absorbent tube was also performed in the summer and as shown in figure (18), which shows a sample of the results obtained in the summer where the mass flow rate of the water entering the solar collector was increased to a value (0.066) kg / s and the test was carried out on 14 May 2019 to obtain similar weather conditions, and the results showed that the thermal efficiency increased significantly with the increase in water flow, while increasing the mass flow rate of the water entering the solar collector reduces the difference in the temperature degrees between the inlet and outlet vents of the absorbent tube, as shown in figure (19), where the temperature difference is observed during the reduction of the mass flow rate of the water entering the tube, and this is also consistent with the results of the winter season, which is mainly due to the same reasons mentioned above.

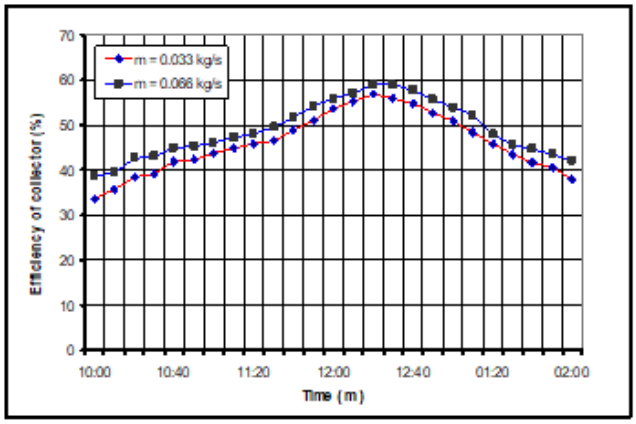

Figure (18) Solar collector efficiency at different mass flow rate of water entering the solar collector for May 2019

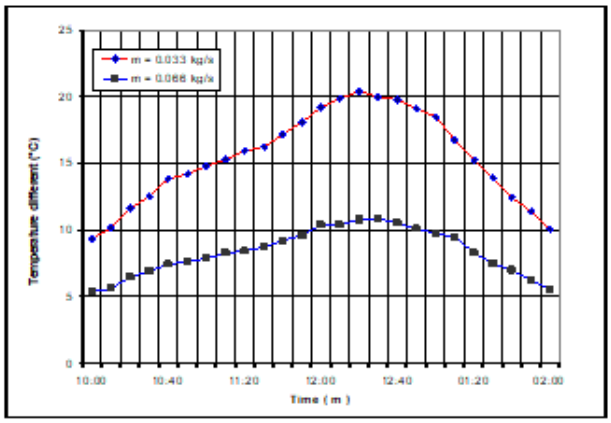

Figure (19) The difference in temperature between the inlet and outlet openings of the absorbent tube at a different mass flow rate of water entering the solar collector for May 2019

7. CONCLUSIONS

In this research, a number of conclusions were reached, namely:

1- Increasing the solar flux increases the useful energy obtained from the solar collector.

2- Increasing the temperature of the water inside the absorbent tube increases the heat losses. Therefore, it is preferable to increase the flow of water through the absorbent tube.

3- Increasing the mass flow rate of the fluid increases the efficiency of the solar collector.

4- Increasing the mass flow rate of the fluid leads to a reduction in the temperature difference between the inlet and the exit area of the fluid.

5- The useful energy obtained from the collectors increased from 10:00 to reach its highest value between 12:00 and 1:00 hours, coinciding with the increase in the solar flux, then it decreases with the decrease in the solar flux. Heat coefficients for both seasons of the year.

6- The best efficiency of the solar collector was between (12:00) and (1:00) in the evening

REFERENCES

[1] Ouagued and Malika,(2011)" Simulation and thermal study of a parabolic Trough Solar Collector" Renewable Energies Development Center CDER, Algiers, Algeria,2nd International Conference on energy conversion and conservation.

[2] Kalogirou, S. A., & Lloyd, S. (1992). Use of solar parabolic trough collectors for hot water production in Cyprus. A feasibility study. Renewable Energy, 2(2), 117-124.

[3] Oommen, R. Y., & Jayaraman, S. (2001). Development and performance analysis of compound parabolic solar concentrators with reduced gap losses–oversized reflector. energy conversion and management, 42(11), 1379-1399.

[4] Morrison, G. L., & Braun, J. E. (1985). System modeling and operation characteristics of thermosyphon solar water heaters. Solar Energy, 34(4-5), 389-405.

[5] Kalogirou, S. (1998). Use of parabolic trough solar energy collectors for sea-water desalination. Applied Energy, 60(2), 65-88.

[6] May, E. K., & Murphy, L. M. (1983). Performance benefits of the direct generation of steam in line-focus solar collectors.,105, pp. 126-133.

[7] Zarza, E., Valenzuela, L., Leo´ n, J., Weyers, H. D., Eickhoff, M., Eck, M., & Hennecke, K. (2002). The DISS project: direct steam generation in parabolic trough systems. Operation and maintenance experience and update on project status. J. Sol. Energy Eng., 124(2), 126-133.

[8] Zarza, E., Valenzuela, L., Leon, J., Hennecke, K., Eck, M., Weyers, H. D., & Eickhoff, M. (2004). Direct steam generation in parabolic troughs: Final results and conclusions of the DISS project. Energy, 29(5-6), 635-644.

[9] García-Rodríguez, L., & Gómez-Camacho, C. (1999). Design parameter selection for a distillation system coupled to a solar parabolic trough collector. Desalination, 122(2-3), 195-204.

[10] García-Rodríguez, L., & Gómez-Camacho, C. (1999). Thermoeconomic analysis of a solar parabolic trough collector distillation plant. Desalination, 122(2-3), 215-224.

[11] Garg, H. P. (2005). Solar energy: fundamentals and applications. Tata McGraw-Hill Education.

[12] Sarker, M. R. I., Beg, M. R. A., Hossain, M. Z., Islam, M. T., & Zaman, M. R. (2005). Design of a Software Controlled Two axis Automatic Solar tracking system. Mech. Eng. Res. Journal, 5.

[13]Hegazy, A. S., & ElMadany, M. M. (2007, November). Design and experimental testing of a solar parabolic trough collector with its tracking system for salt-water desalination in arid areas of Saudi Arabia. In Proceedings, 7th Saudi Engineering Conference (pp. 02-05).

[14] Dagan, E., Muller, M., & Lippke, F. (1992). Direct steam generation in the parabolic trough collector. Report of Platafoma Solar de Almeria, Madrid.

[15] Lippke, F. (1996). Direct steam generation in parabolic trough solar power plants: numerical investigation of the transients and the control of a once-through system.

[16] Kalogirou, S. (1996). Parabolic trough collector system for low temperature steam generation: design and performance characteristics. Applied Energy, 55(1), 1-19.

[17] Ibrahim, S. M. (1996). The forced circulation performance of a sun tracking parabolic concentrator collector. Renewable energy, 9(1-4), 568-571.

[18] Almanza, R., Lentz, A., & Jimenez, G. (1997). Receiver behavior in direct steam generation with parabolic troughs. *Solar Energy*, *61*(4), 275-278.

[19] Bakos, G. C., Adamopoulos, D., Tsagas, N. F., & Soursos, M. (1999). Design and construction of a line-focus parabolic trough solar concentrator for electricity generation. In Proceedings of ISES solar world congress, Jerusalem (p. 16).

[20] Singh, B., & Sulaiman, F. (2001). Hfactor To Determine The Convective Heat Transfer Coefficient Of Saturated Water Flowing In Tubes. Persidangan Fizik Kebangsaan (PERFIK 2001), jointly organized by the Physics Institute of Malaysia and University Malaya.

[21] Kulkarni MH, Shinde NN(2008). Design, Construction and Review of Thermal Performance of Closed Cylindrical Parabolic Trough.

[22] Yassen, T. A. (2012). Experimental and theoretical study of a parabolic trough solar collector. Anbar J. Eng. Sci, 5(1), 109-125.

[23] Incropera, F. P., Lavine, A. S., Bergman, T. L., & DeWitt, D. P. (2011). Fundamentals of heat and mass transfer.Wiley.

P- ISSN 1991-8941E-ISSN 2706-6703 *Journal of University of Anbar for Pure Science (JUAPS)* Open Access
2021,15 (1) :38 – 49

دراسة عملية ونظرية لأداء مجمع شمسي نوع قطع مكافئ بدون نظام تعقب أوتوماتيكي

خضر زيدان زراك[1],.فياض محمد عبد[2] , سالم يحيى قاسم[2]
[1] مديريه مجاري الانبار- محافظة الانبار, الرمادي , العراق
[2] قسم الهندسة الميكانيكية, كلية الهندسة , جامعة تكريت , تكريت ,العراق

الخلاصة

في هذا البحث أجريت دراسة عملية ونظرية لتقييم معاملات الأداء لمجمع شمسي حوضي نوع قطع مكافئ (PTCS) بطول (3 m) وعرض (2.67 m) ولثلاثة لواقط مربوطة على التوازي، وأنبوب ماص (Absorber tube) مصنوع من الفولاذ (Stainless steel) قطره الداخلي (0.028 m) والخارجي (0.031 m) وطوله (11 m) ربط على التوالي, تم طلاءه بطلاء اسود غير لماع لكي يزيد من امتصاص أشعة الشمس ويقلل من الإشعاع الحراري للأنبوب الماص, يجري المائع خلال الأنبوب الواقع في بؤرة اللواقط الثلاثة ما بين فتحتي الدخول والخروج, عرض اللاقط (Aperture width) (0.8) متر وطوله (2.40) متر وزاوية حافة (Rim angle) (Ø= 90°) ونسبة تركيز (Concentration ratio) (25.19). سطح اللاقط تم اكساءه بمادة من ورق الألمنيوم (رقائق الألمنيوم) المتوفرة في الأسواق المحلية (3M SA-85) والتي تغطي صفائح الحديد المغلون سمكها (2 ملم). تم بناء برنامج حاسوبي بلغة فورتران لحساب الأداء للمجمع الشمسي. أوضحت النتائج العملية لهذا الاختبار أن منحني الأداء للمجمع منخفضاً انخفاضاً ملحوظاً عن منحني أداء المجمع النموذجي المماثل حيث يلاحظ وجود حيود كبير ما بين النتائج النظرية والعملية وبالأخص في فصل الشتاء, إذ بلغ الحيود عند الساعة العاشرة صباحاً نسبة (78 %) بينما بلغ الحيود عند الساعة الثانية عشراً حوالي (5 %). إن نسبة الحيود المذكورة تعود إلى الافتراضيات التي تم وضعها لتبسيط حل المعادلات التي تم استخدامها في الجانب النظري من البحث وكذلك ويعزو السبب إلى أن النتائج النظرية تؤخذ على افتراض أن الظروف الجوية جيدة والسماء صافية وهذا على عكس الواقع الموجود في فصل الشتاء, أن أفضل كفاءة للمجمع الشمسي كانت مابين الساعة (12:00) والساعة (1:00) مساءاً ولكلا الفصلين. كما أوضحت النتائج التي حصلنا عليها أن زيادة معدل التدفق الكتلي للمائع من مقدار (0.033) كغم/ ثانية إلى مقدار(0.066) كغم/ ثانية يزيد من كفاءة المجمع الشمسي.